

Search for Violations of Lorentz Invariance and *CPT* Symmetry in $B_{(s)}^0$ Mixing

R. Aaij *et al.*^{*}

(LHCb Collaboration)

(Received 16 March 2016; published 15 June 2016)

Violations of *CPT* symmetry and Lorentz invariance are searched for by studying interference effects in B^0 mixing and in B_s^0 mixing. Samples of $B^0 \rightarrow J/\psi K_S^0$ and $B_s^0 \rightarrow J/\psi K^+ K^-$ decays are recorded by the LHCb detector in proton-proton collisions at center-of-mass energies of 7 and 8 TeV, corresponding to an integrated luminosity of 3 fb^{-1} . No periodic variations of the particle-antiparticle mass differences are found, consistent with Lorentz invariance and *CPT* symmetry. Results are expressed in terms of the standard model extension parameter Δa_μ with precisions of $\mathcal{O}(10^{-15})$ and $\mathcal{O}(10^{-14})$ GeV for the B^0 and B_s^0 systems, respectively. With no assumption on Lorentz (non)invariance, the *CPT*-violating parameter z in the B_s^0 system is measured for the first time and found to be $\mathcal{R}e(z) = -0.022 \pm 0.033 \pm 0.005$ and $\mathcal{I}m(z) = 0.004 \pm 0.011 \pm 0.002$, where the first uncertainties are statistical and the second systematic.

DOI: 10.1103/PhysRevLett.116.241601

Lorentz invariance and the combination of charge conjugation, spatial inversion, and time reversal (*CPT*) are exact symmetries in the standard model (SM) of particle physics, and are deeply connected in any quantum field theory [1]. Quantum theories that aim to describe Planck-scale physics, such as string theory, might break these fundamental symmetries [2]. Present-day experiments are many orders of magnitude away from the Planck energy scale of $\sim 10^{19}$ GeV; however, small effects at low energy might still be observable. Interference effects in the mixing of neutral mesons are sensitive to violations of *CPT* symmetry, and therefore may provide a window to the quantum gravity scale [3]. Such effects can be quantified in a low-energy, effective field theory, as done in the standard model extension (SME) [4,5]. In this framework, terms that explicitly break Lorentz and *CPT* symmetry are added to the SM Lagrangian to describe the couplings between particles and (hypothetical) uniform tensor fields. These fields would acquire nonzero vacuum expectation values when these symmetries are spontaneously broken in the underlying theory. The SME couplings are expected to be suppressed by powers of the Planck scale [6]. In the SME, the *CPT* -violating parameters that can be measured in neutral meson systems also break Lorentz symmetry. The amount of *CPT* violation depends on the direction of motion and on the boost of the particle. The SME parameters for the B^0 and B_s^0 systems can be best measured with a time-dependent analysis of the decay channels $B^0 \rightarrow J/\psi K_S^0$ and $B_s^0 \rightarrow J/\psi K^+ K^-$, using the four-velocity of the

B mesons [7]. The notation B refers to either B^0 or B_s^0 and the inclusion of charge-conjugate processes is implied throughout this Letter. These parameters have been measured previously, albeit with less sensitive decay modes [7], by the *BABAR* collaboration for the B^0 system [8], and by the D0 collaboration for the B_s^0 system [9].

The LHCb detector is a single-arm forward spectrometer described in detail in Refs. [10,11]. Simulated events are produced using the software described in Refs. [12–16]. The data used in this analysis correspond to an integrated luminosity of 3 fb^{-1} , taken at the LHC at proton-proton center-of-mass energies of 7 and 8 TeV. The selection of both decay channels is the same as used in Refs. [17] and [18]. The J/ψ meson is reconstructed in the dimuon channel and the K_S^0 meson in the $\pi^+ \pi^-$ final state.

Interference effects from *CPT* violation can be incorporated generically in the time evolution of a neutral B meson system, described by the Schrödinger equation $i\partial_t \Psi = \hat{H}\Psi$. The effective 2×2 Hamiltonian is written as $\hat{H} = \hat{M} - i\hat{\Gamma}/2$ [19]. Diagonalization gives a heavy-mass eigenstate $|B_H\rangle$ and a light-mass eigenstate $|B_L\rangle$ with masses $m_{H,L}$ and decay widths $\Gamma_{H,L}$. The differences between the eigenvalues are defined as $\Delta m \equiv m_H - m_L$ and $\Delta\Gamma \equiv \Gamma_L - \Gamma_H$. The differences between the diagonal matrix elements of the effective Hamiltonian are defined as $\delta m \equiv M_{11} - M_{22}$ and $\delta\Gamma \equiv \Gamma_{11} - \Gamma_{22}$. Any difference between the mass or lifetime of particles and antiparticles (i.e., a nonzero δm or $\delta\Gamma$) is a sign of *CPT* violation, and is characterized by

$$z = \frac{\delta m - i\delta\Gamma/2}{\Delta m + i\Delta\Gamma/2}, \quad (1)$$

and the mass eigenstates are given by $|B_{H,L}\rangle = p\sqrt{1 \pm z}|B\rangle \mp q\sqrt{1 \mp z}|\bar{B}\rangle$. Owing to the smallness of the B mixing parameters Δm and $\Delta\Gamma$ in the denominator, z is highly sensitive to *CPT*-violating effects.

*Full author list given at the end of the article.

TABLE I. Time-dependent functions $h_k(t)$ in Eq. (4).

k	$h_k(t)$
1	$ A_0(t) ^2$
2	$ A_{\parallel}(t) ^2$
3	$ A_{\perp}(t) ^2$
4	$\mathcal{Im}[A_{\parallel}^*(t)A_{\perp}(t)]$
5	$\mathcal{Re}[A_0^*(t)A_{\parallel}(t)]$
6	$\mathcal{Im}[A_0^*(t)A_{\perp}(t)]$
7	$ A_S(t) ^2$
8	$\mathcal{Re}[A_S^*(t)A_{\parallel}(t)]$
9	$\mathcal{Im}[A_S^*(t)A_{\perp}(t)]$
10	$\mathcal{Re}[A_S^*(t)A_0(t)]$

Considering only contributions to first order in z , the decay rate to a CP eigenstate f as a function of the B proper decay time t becomes

$$\begin{aligned} \frac{d\Gamma_f}{dt} \propto & e^{-\Gamma t} \{ [1 + \zeta D_f \mathcal{Re}(z) - S_f \mathcal{Im}(z)] \cosh(\Delta\Gamma t/2) \\ & + [D_f + \mathcal{Re}(z)(C_f + \zeta)] \sinh(\Delta\Gamma t/2) \\ & + \zeta [C_f - D_f \mathcal{Re}(z) + \zeta S_f \mathcal{Im}(z)] \cos(\Delta m t) \\ & - \zeta [S_f - \mathcal{Im}(z)(C_f + \zeta)] \sin(\Delta m t) \}, \end{aligned} \quad (2)$$

where $\Gamma \equiv (\Gamma_{11} + \Gamma_{22})/2$, $\zeta = +1(-1)$ for an initial $|B\rangle$ ($|\bar{B}\rangle$) state and the following definitions are introduced:

$$\begin{aligned} C_f &\equiv \frac{1 - |\lambda_f|^2}{1 + |\lambda_f|^2}, & S_f &\equiv \frac{2\mathcal{Im}(\lambda_f)}{1 + |\lambda_f|^2}, \\ D_f &\equiv -\frac{2\mathcal{Re}(\lambda_f)}{1 + |\lambda_f|^2}, & \lambda_f &\equiv \frac{q\bar{A}_f}{pA_f}, \end{aligned} \quad (3)$$

with A_f and \bar{A}_f being the direct decay amplitudes of a $|B\rangle$ or $|\bar{B}\rangle$ state to the eigenstate f .

For the decay $B^0 \rightarrow J/\psi K_S^0$, the final state is CP odd, corresponding to the CP eigenvalue $\eta_f = -1$. In the SM, $\arg(\lambda_{J/\psi K_S^0}) = \pi - 2\beta$, where β is defined in terms of elements of the CKM matrix as $\beta \equiv \arg[-(V_{cd}V_{cb}^*)/(V_{td}V_{tb}^*)]$. Furthermore, in the B^0 system, the approximation $\Delta\Gamma_d = 0$ is made, as supported by experimental data [20].

TABLE II. Definition of the coefficients in Eq. (5). The following definitions are used: $\eta^+ \equiv (1 + \eta_l\eta_m)/2$, $\eta^- \equiv (1 - \eta_l\eta_m)/2$, $\eta^{\mathcal{Im}} \equiv i(\eta_l - \eta_m)/2$, $\eta^{\mathcal{Re}} \equiv (\eta_l + \eta_m)/2$. Furthermore, $\zeta^+ \equiv (\zeta)^{\eta^+}$, and $\zeta^- \equiv (\zeta)^{\eta^-}$, such that $\zeta^{\pm} = 1$ if $\eta^{\pm} = 0$ and $\zeta^{\pm} = \zeta$ otherwise.

$$\begin{aligned} a_k &= (\eta^+ + \eta^- C_f) + \zeta \mathcal{Re}(z)(\eta^{\mathcal{Re}} D_f + \eta^{\mathcal{Im}} S_f) + \mathcal{Im}(z)(\eta^{\mathcal{Im}} D_f - \eta^{\mathcal{Re}} S_f) \\ b_k &= (\eta^{\mathcal{Re}} D_f + \eta^{\mathcal{Im}} S_f) + \mathcal{Re}(z)(\zeta^+ + \zeta^- C_f) \\ c_k &= \zeta(\eta^- + \eta^+ C_f) - \zeta \mathcal{Re}(z)(\eta^{\mathcal{Re}} D_f + \eta^{\mathcal{Im}} S_f) - \mathcal{Im}(z)(\eta^{\mathcal{Im}} D_f - \eta^{\mathcal{Re}} S_f) \\ d_k &= \zeta(\eta^{\mathcal{Im}} D_f - \eta^{\mathcal{Re}} S_f) + \mathcal{Im}(z)(\zeta^+ + \zeta^- C_f) \end{aligned}$$

The decay $B_s^0 \rightarrow J/\psi K^+ K^-$ is similar to $B^0 \rightarrow J/\psi K_S^0$, but the decay width difference $\Delta\Gamma_s$ cannot be ignored [20]. Another important difference is that the $K^+ K^-$ system mostly originates from the $\phi(1020)$ resonance, giving the $K^+ K^-$ pair an orbital angular momentum $L = 1$ (P wave). Since the $J/\psi \phi$ final state consists of two vector mesons, its orbital angular momentum can be $L \in \{0, 1, 2\}$ for the polarization states $f \in \{0, \perp, \parallel\}$, respectively, with corresponding CP eigenvalues $\eta_f = (-1)^L$. The $K^+ K^-$ system has a small S -wave contribution [18], which results in another $L = 1$ component for the $J/\psi K^+ K^-$ final state. These four polarization states can be separated statistically in the helicity formalism [21], using the three decay angles between the final-state particles. The corresponding weak phases, $\arg(\lambda_{J/\psi K^+ K^-}) = L\pi - \phi_s$, can, in the SM, be expressed in terms of CKM matrix elements, $\phi_s = -2\beta_s \equiv -2\arg[-(V_{ts}V_{tb}^*)/(V_{cs}V_{cb}^*)]$. The decay rate has to be modified compared to Eq. (2) to include the angular dependence. It becomes a sum over all ten combinations of the four helicity amplitudes,

$$\frac{d^4\Gamma_{J/\psi K^+ K^-}}{dt d\vec{\Omega}} \propto \sum_{k=1}^{10} h_k(t) f_k(\vec{\Omega}), \quad (4)$$

where $f_k(\vec{\Omega})$ are angular functions, given in Ref. [21], and $h_k(t)$ are products of the amplitudes as listed in Table I. The time dependence of $h_k(t)$ is given by

$$\begin{aligned} A_l^*(t) A_m(t) &= \frac{A_l^*(0) A_m(0) e^{-\Gamma_s t}}{1 + \zeta C_f} \\ &\times [a_k \cosh(\Delta\Gamma_s t/2) + b_k \sinh(\Delta\Gamma_s t/2) \\ &+ c_k \cos(\Delta m_s t) + d_k \sin(\Delta m_s t)], \end{aligned} \quad (5)$$

with the coefficients listed in Table II.

In the SME, the dimensionless parameter z is not a constant. It depends on the four-velocity $\beta^\mu = (\gamma, \vec{\beta})$ of the neutral meson as [22,23]

$$z = \frac{\beta^\mu \Delta a_\mu}{\Delta m + i\Delta\Gamma/2}, \quad (6)$$

thereby breaking Lorentz invariance. The SME parameter Δa_μ describes the difference between the couplings of the

valence quarks, within the neutral meson, with the Lorentz-violating fields [22]. Therefore, B^0 and B_s^0 mesons can have different values of Δa_μ . Since Δa_μ is real [24], it follows that $\mathcal{R}e(z)\Delta\Gamma = -2\mathcal{I}m(z)\Delta m$. For B mesons, $\Delta m \gg \Delta\Gamma$, and so $\mathcal{I}m(z)$ is 2 orders of magnitude smaller than $\mathcal{R}e(z)$, and can be ignored in the measurements of Δa_μ . The average boost of B mesons in the acceptance of LHCb is $\langle\gamma\beta\rangle \approx 20$. It follows from Eq. (6) that this large boost results in a high sensitivity to Δa_μ [7].

To measure Δa_μ , the meson direction needs to be determined in an absolute reference frame. Such a frame can be defined with respect to fixed stars [24]. In this frame, the Z axis points north along Earth's rotation axis, the X axis points from the Sun to the vernal equinox on January 1, 2000 (J2000 epoch), and the Y axis completes the right-handed coordinate system. The latitude of the LHCb interaction point is 46.2414°N , the longitude is 6.0963°E , and the angle of the beam east of north is 236.296° . The beam axis is inclined with respect to the geodetic plane by 3.601 mrad, pointing slightly upwards. The timekeeping has been obtained from the LHC machine with a time stamp, t_{LHC} , in UTC microseconds since January 1, 1970, 00:00:00 UTC. The time, spatial coordinates, and angles have negligible uncertainties and are used to define the rotation from the coordinate system of LHCb to the absolute reference frame. For mesons traveling along the beam axis, $\mathcal{R}e(z)$ can be expressed as

$$\begin{aligned}\mathcal{R}e(z) &= \frac{\Delta m}{\Delta m^2 + \Delta\Gamma^2/4} \beta^\mu \Delta a_\mu \\ &\approx \frac{\gamma}{\Delta m} \{ \Delta a_0 + \cos(\chi) \Delta a_Z \\ &\quad + \sin(\chi) [\Delta a_Y \sin(\Omega\hat{t}) + \Delta a_X \cos(\Omega\hat{t})] \},\end{aligned}\quad (7)$$

where $|\vec{\beta}|$ is set to unity, $\Delta a^{X,Y,Z} = -\Delta a_{X,Y,Z}$, and $\chi = 112.4^\circ$ is the angle between the beam axis and the rotational axis of Earth. The time dependence results from the Earth's rotation, giving a periodicity with sidereal frequency Ω . The sidereal phase at $t_{\text{LHC}} = 0$ is found to be $\hat{t} = (2.8126 \pm 0.0014)$ hr. The B mesons are emitted at an average angle of about 5° from the beam axis. This means that the LHCb detector is mostly sensitive to the linear combination $\Delta a_{||} \equiv \Delta a_0 + \cos(\chi) \Delta a_Z = \Delta a_0 - 0.38 \Delta a_Z$, while there is a much weaker sensitivity to the orthogonal parameter, $\Delta a_{\perp} = 0.38 \Delta a_0 + \Delta a_Z$, coming from the smaller transverse component of the B velocity. Both $\Delta a_{||}$ and Δa_{\perp} are measured and the correlation between them is negligible.

Unbinned likelihood fits are applied to the decay-time distributions using Eqs. (2) and (4). To obtain the SME parameters, the sidereal variation of $\mathcal{R}e(z)$ is taken into account by including in the fits the LHC time and the three-momentum of the reconstructed B candidate. For the B_s^0 sample, the fits are performed to the full angular distribution.

In the invariant mass distributions of the B candidates, the background is mostly combinatorial. For both decay channels, this background is statistically subtracted using the sPlot technique [25], which allows us to project out the signal component by weighting each event depending on the mass of the B candidate. The mass models are the same as in Refs. [17,18]. The correlation between the shape of the invariant mass distribution and the B momentum or, for the B_s^0 sample, the decay angles, leads to a small systematic bias for both samples. This effect is included in the systematic uncertainty. In the $B_s^0 \rightarrow J/\psi K^+ K^-$ sample, there is a small contribution coming from misidentified $B^0 \rightarrow J/\psi K^+ \pi^-$ and $\Lambda_b^0 \rightarrow J/\psi p K^-$ decays. This background contribution is statistically removed by adding simulated decays with negative weights. A systematic uncertainty is assigned to account for the uncertainty on the size and shape of this background.

The description of the detection efficiency as a function of the decay time, the decay-time resolution model, and the flavor tagging (to distinguish initial B and \bar{B} mesons) are the same as in Refs. [17] and [18] for the $B^0 \rightarrow J/\psi K_S^0$ and $B_s^0 \rightarrow J/\psi K^+ K^-$ samples, respectively. This description includes the dilution of the asymmetry due to wrong decisions of the flavor tagging method. The decay-time resolution model and tagging calibration do not lead to a systematic bias in the final result. A possible wrong assignment of the primary interaction vertex (PV) to the B candidate gives a small bias in the $\Delta a_{\perp}^{B^0}$ parameter, which is included in the systematic uncertainty. The inefficiency at high decay times, caused by the reconstruction algorithms, is described by an exponential function. For the B^0 sample, this function is obtained from simulation and does not lead to a systematic bias in the result. For the B_s^0 sample, the exponential function is obtained from a data-driven method. The change in the final result when using the correction procedure from Ref. [18] is taken as a systematic uncertainty.

The production asymmetry between B^0 and \bar{B}^0 mesons is included in the modeling of the decay rates, and is taken from Refs. [26,27]. The corresponding uncertainties are included in the statistical uncertainty, while a possible momentum dependence of the production asymmetry is considered as a systematic uncertainty. The B_s^0 production asymmetry does not affect the fit to the B_s^0 sample, since the fast B_s^0 oscillations wash out this effect and the decay rates for B_s^0 and \bar{B}_s^0 tags are normalized separately.

In the fit to the B^0 sample, the correlation between $\mathcal{R}e(z^{B^0})$ and $C_{J/\psi K_S^0}$ is too large to allow determination of $\mathcal{R}e(z^{B^0})$ without making assumptions about the value of $C_{J/\psi K_S^0}$ [7]. On the other hand, to determine $\Delta a_\mu^{B^0}$, the averages $C_{J/\psi K_S^0} = 0.005 \pm 0.020$ and $S_{J/\psi K_S^0} = 0.676 \pm 0.021$ [19] as measured by the *BABAR* and *Belle* collaborations can be used in the fit. Since the boost

of the B^0 mesons is about 40 times lower in these experiments, these values are hardly affected by possible Lorentz violation in the SME. The value of $D_{J/\psi K_s^0}$ is by definition

$\sqrt{1 - S_{J/\psi K_s^0}^2 - C_{J/\psi K_s^0}^2}$. The uncertainties on these external input values are propagated as systematic uncertainties on $\Delta a_\mu^{B^0}$. The mass difference, $\Delta m_d = 0.510 \pm 0.003 \text{ ps}^{-1}$ [19], is allowed to vary in the fit within its uncertainty using a Gaussian constraint. Setting $\Delta\Gamma_d = 0.007 \text{ ps}^{-1}$, which corresponds to the experimental uncertainty [20], leads to a small change in $\Delta a_\parallel^{B^0}$, which is included in the systematic uncertainty. The B^0 lifetime is allowed to vary freely in the fit.

In the fit to the B_s^0 sample, the correlation between $\mathcal{R}(z^{B_s^0})$ and $C_{J/\psi K^+ K^-}$ is small owing to the additional interference terms from the helicity amplitudes, the nonzero $\Delta\Gamma_s$, and the faster $B_s^0 - \bar{B}_s^0$ oscillations. For this reason, the same parameters as in Ref. [18] are varied freely in the fit, in addition to either Δa_μ or z . The detection efficiency is also described as a function of the decay angles. The shape of this angular acceptance is obtained from simulation. The simulated events are weighted to match the kinematic distributions in data. The uncertainty due to the limited number of simulated events and the full effect of correcting for the kinematic distributions in data are added to the systematic uncertainty. Systematic effects due to the decay-angle resolution are negligibly small. The fit to the B_s^0 sample is performed simultaneously in bins of the $K^+ K^-$ invariant mass [18]. Each bin has a different interference between the P - and S -wave amplitudes. This effect is included in the fit and no systematic biases are observed.

An overview of the systematic uncertainties is given in Table III. For the B^0 mixing, the largest contribution comes from the uncertainty on the external parameters C_f and S_f . A small systematic bias is observed in $\Delta a_\perp^{B^0}$ due to the momentum dependence of the cross sections of neutral kaons in the detector material. For the B_s^0 mixing, the largest contribution comes from the description of the decay-time acceptance. Effects from the correlation between the mass and decay time and from the accuracy of the length scale and momentum scale of the detector are found to be negligible.

The components of the SME parameter Δa_μ for B^0 mixing, obtained from the fit to the sample of selected $B^0 \rightarrow J/\psi K_s^0$ candidates, are

$$\begin{aligned}\Delta a_\parallel^{B^0} &= [-0.10 \pm 0.82(\text{stat}) \pm 0.54(\text{syst})] \times 10^{-15} \text{ GeV}, \\ \Delta a_\perp^{B^0} &= [-0.20 \pm 0.22(\text{stat}) \pm 0.04(\text{syst})] \times 10^{-13} \text{ GeV}, \\ \Delta a_X^{B^0} &= [+1.97 \pm 1.30(\text{stat}) \pm 0.29(\text{syst})] \times 10^{-15} \text{ GeV}, \\ \Delta a_Y^{B^0} &= [+0.44 \pm 1.26(\text{stat}) \pm 0.29(\text{syst})] \times 10^{-15} \text{ GeV},\end{aligned}$$

and the corresponding numbers for B_s^0 mixing, using $B_s^0 \rightarrow J/\psi K^+ K^-$ candidates, are

TABLE III. Systematic uncertainties on Δa_μ for B^0 mixing and on Δa_μ and z for B_s^0 mixing. Contributions marked with centered dots are negligible.

B^0 mixing	Δa_\parallel	Δa_\perp	$\Delta a_{X,Y}$		
Source	$[\times 10^{-15} \text{ GeV}]$				
Mass correlation	0.04		
Wrong PV assignment	...	1	...		
Production asymmetry	0.28	1	0.05		
External input C_f, S_f	0.46	4	0.28		
Decay width difference	0.07		
Neutral kaon asymmetry	...	1	...		
Quadratic sum	0.54	4	0.29		

B_s^0 mixing	Δa_\parallel	Δa_\perp	$\Delta a_{X,Y}$	$\mathcal{R}(z)$	$\mathcal{I}(z)$
Source	$[\times 10^{-14} \text{ GeV}]$				
Mass correlation	0.10	3	0.24	0.001	0.002
Peaking background	0.14	3	0.15	0.003	...
Decay-time acceptance	0.30	7	0.65	...	0.001
Angular acceptance	0.07	0.002	0.001
Quadratic sum	0.36	8	0.71	0.003	0.002

$$\begin{aligned}\Delta a_\parallel^{B_s^0} &= [-0.89 \pm 1.41(\text{stat}) \pm 0.36(\text{syst})] \times 10^{-14} \text{ GeV}, \\ \Delta a_\perp^{B_s^0} &= [-0.47 \pm 0.39(\text{stat}) \pm 0.08(\text{syst})] \times 10^{-12} \text{ GeV}, \\ \Delta a_X^{B_s^0} &= [+1.01 \pm 2.08(\text{stat}) \pm 0.71(\text{syst})] \times 10^{-14} \text{ GeV}, \\ \Delta a_Y^{B_s^0} &= [-3.83 \pm 2.09(\text{stat}) \pm 0.71(\text{syst})] \times 10^{-14} \text{ GeV}.\end{aligned}$$

Figure 1 shows the result of fits of $\mathcal{R}(z)$ in bins of the sidereal phase for both samples. For the B^0 sample, the external constraints on $C_{J/\psi K_s^0}$ and $S_{J/\psi K_s^0}$ are again used. No sidereal variation is observed. Independently of any

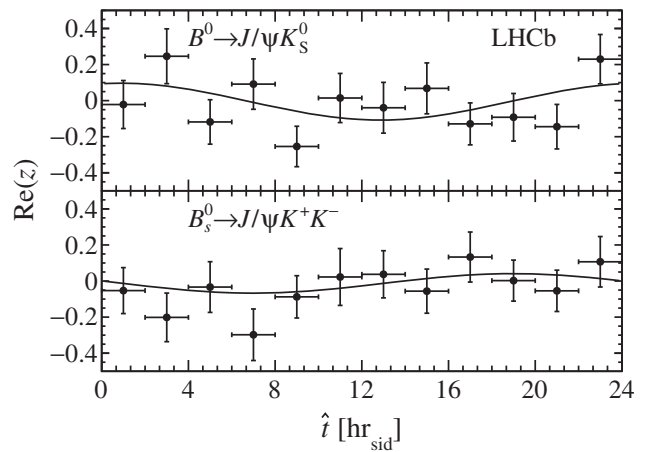


FIG. 1. Values of $\mathcal{R}(z)$ obtained from fits in bins of sidereal phase for (top) the B^0 sample and (bottom) the B_s^0 sample. The solid line shows the variation of $\mathcal{R}(z)$ from the Δa_μ fits, using the average B momentum.

assumption of Lorentz violation, the complex *CPT*-violating parameter z in the B_s^0 system is found to be

$$\begin{aligned}\mathcal{R}e(z^{B_s^0}) &= -0.022 \pm 0.033(\text{stat}) \pm 0.003(\text{syst}), \\ \mathcal{I}m(z^{B_s^0}) &= 0.004 \pm 0.011(\text{stat}) \pm 0.002(\text{syst}).\end{aligned}$$

Since the SME fits consider only one specific frequency, i.e., the sidereal frequency, a wide range of frequencies is scanned by means of the periodogram method. A periodogram gives the spectral power $P(\nu)$ of a frequency ν in a signal sampled at discrete, not necessarily equidistant, times. In this analysis, the Lomb-Scargle periodogram [28] is used, as in the *BABAR* measurement of $\Delta a_\mu^{B^0}$ [8].

The periodogram is determined for the term in the decay rates proportional to $e^{-\Gamma t} \mathcal{R}e(z)$. Since negative weights cannot be used in the periodogram, the B mass windows are narrowed to $5260 < m_{J/\psi K_S^0} < 5300 \text{ MeV}/c^2$ and $5350 < m_{J/\psi K^+ K^-} < 5390 \text{ MeV}/c^2$ compared to those used in the fits [17,18]. In total about 5200 frequencies are scanned in a wide range around the sidereal frequency, from 0.03 to 2.10 solar day $^{-1}$. The number of frequencies oversamples the number of independent frequencies by roughly a factor of 2, thereby avoiding any undersampling [29]. As the data are unevenly sampled, the false-alarm probability is determined from simulation [29], where the time stamps are taken from data.

The two periodograms are shown in Fig. 2. No significant peaks are found. For the B^0 periodogram, the highest peak $P(\nu_{\max}) = 8.09$ is found at a frequency of 1.5507 solar day $^{-1}$ and has a false-alarm probability of 0.57. There are 2707 (1559) sampled frequencies with a larger spectral power than the peak at the sidereal (solar) frequency. For the B_s^0

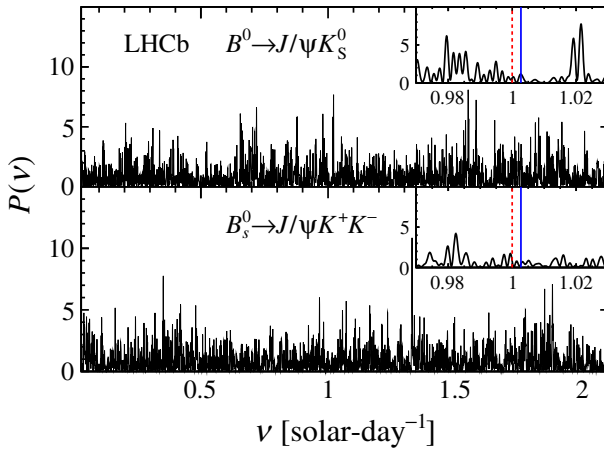


FIG. 2. Periodograms for (top) the B^0 and (bottom) B_s^0 sample. The insets show a zoom around the solar (red dashed line) and sidereal (blue solid line) frequencies, which have been made by highly oversampling the frequencies in this narrow range.

periodogram the highest peak $P(\nu_{\max}) = 10.85$ is found at a frequency of 1.3301 solar day $^{-1}$ and has a false-alarm probability of 0.06. There are 3386 (2356) frequencies with a larger spectral power than the sidereal (solar) peak. The absence of any signal in the SME fits is confirmed by the absence of significant peaks at the sidereal frequency.

The results presented here are consistent with *CPT* symmetry and Lorentz invariance. The measurement of $\Delta a_\mu^{B^0}$ is an improvement in precision of about 3 orders of magnitude compared to the one from the *BABAR* collaboration [8] when the SM prediction $\Delta \Gamma_d = -0.0027 \text{ ps}^{-1}$ [30] is used to scale their result. The measurement of $\Delta a_\mu^{B_s^0}$ is an order of magnitude more precise than the one from the D0 collaboration [9] (note the different definition, $\Delta a_\perp \equiv \sqrt{\Delta a_X^2 + \Delta a_Y^2}$, in Ref. [9]). The measurement of $z^{B_s^0}$ is the first direct measurement of this quantity.

We express our gratitude to our colleagues in the CERN accelerator departments for the excellent performance of the LHC. We thank the technical and administrative staff at the LHCb institutes. We acknowledge support from CERN and from the following national agencies: CAPES, CNPq, FAPERJ, and FINEP (Brazil); NSFC (China); CNRS/IN2P3 (France); BMBF, DFG, and MPG (Germany); INFN (Italy); FOM and NWO (Netherlands); MNiSW and NCN (Poland); MEN/IFA (Romania); MinES and FANO (Russia); MinECo (Spain); SNSF and SER (Switzerland); NASU (Ukraine); STFC (United Kingdom); and NSF (USA). We acknowledge the computing resources that are provided by CERN, IN2P3 (France); KIT and DESY (Germany); INFN (Italy); SURF (Netherlands); PIC (Spain); GridPP (United Kingdom); RRCKI and Yandex LLC (Russia); CSCS (Switzerland); IFIN-HH (Romania); CBPF (Brazil); PL-GRID (Poland); and OSC (USA). We are indebted to the communities behind the multiple open source software packages on which we depend. Individual groups or members have received support from AvH Foundation (Germany); EPLANET; Marie Skłodowska-Curie Actions and ERC (European Union); Conseil Général de Haute-Savoie; Labex ENIGMASS and OCEVU; Région Auvergne (France); RFBR and Yandex LLC (Russia); GVA, XuntaGal, and GENCAT (Spain); Herchel Smith Fund; the Royal Society, Royal Commission for the Exhibition of 1851, and the Leverhulme Trust (United Kingdom).

-
- [1] O. W. Greenberg, *Phys. Rev. Lett.* **89**, 231602 (2002).
 - [2] V. A. Kostelecký and S. Samuel, *Phys. Rev. D* **39**, 683 (1989).
 - [3] S. Liberati, *Classical Quantum Gravity* **30**, 133001 (2013).
 - [4] D. Colladay and V. A. Kostelecký, *Phys. Rev. D* **55**, 6760 (1997).
 - [5] D. Colladay and V. A. Kostelecký, *Phys. Rev. D* **58**, 116002 (1998).

- [6] V. A. Kostelecký and R. Potting, *Nucl. Phys.* **B359**, 545 (1991); V. A. Kostelecký and R. Potting, *Phys. Rev. D* **51**, 3923 (1995).
- [7] J. van Tilburg and M. van Veghel, *Phys. Lett. B* **742**, 236 (2015).
- [8] B. Aubert *et al.* (*BABAR* Collaboration), *Phys. Rev. Lett.* **100**, 131802 (2008).
- [9] V. M. Abazov *et al.* (*D0* Collaboration), *Phys. Rev. Lett.* **115**, 161601 (2015); V. M. Abazov *et al.* (*D0* Collaboration), *Phys. Rev. Lett.* **116**, 019901 (2016).
- [10] A. A. Alves, Jr. *et al.* (*LHCb* Collaboration), *J. Instrum.* **3**, S08005 (2008).
- [11] R. Aaij *et al.* (*LHCb* Collaboration), *Int. J. Mod. Phys. A* **30**, 1530022 (2015).
- [12] T. Sjöstrand, S. Mrenna, and P. Skands, *J. High Energy Phys.* **05** (2006) 026; T. Sjöstrand, S. Mrenna, and P. Skands, *Comput. Phys. Commun.* **178**, 852 (2008).
- [13] I. Belyaev *et al.*, *J. Phys. Conf. Ser.* **331**, 032047 (2011).
- [14] D. J. Lange, *Nucl. Instrum. Methods Phys. Res., Sect. A* **462**, 152 (2001).
- [15] J. Allison, K. Amako, J. Apostolakis, H. Araujo, P. Dubois *et al.* (*Geant4* Collaboration), *IEEE Trans. Nucl. Sci.* **53**, 270 (2006); S. Agostinelli *et al.* (*Geant4* Collaboration), *Nucl. Instrum. Methods Phys. Res., Sect. A* **506**, 250 (2003).
- [16] M. Clemencic, G. Corti, S. Easo, C. R. Jones, S. Miglioranzi, M. Pappagallo, and P. Robbe, *J. Phys. Conf. Ser.* **331**, 032023 (2011).
- [17] R. Aaij *et al.* (*LHCb* Collaboration), *Phys. Rev. Lett.* **115**, 031601 (2015).
- [18] R. Aaij *et al.* (*LHCb* Collaboration), *Phys. Rev. Lett.* **114**, 041801 (2015).
- [19] K. A. Olive *et al.* (Particle Data Group), *Chin. Phys.* **C38**, 090001 (2014).
- [20] Y. Amhis *et al.* (Heavy Flavor Averaging Group), arXiv: 1412.7515.
- [21] R. Aaij *et al.* (*LHCb* Collaboration), *Phys. Rev. D* **87**, 112010 (2013).
- [22] V. A. Kostelecký, *Phys. Rev. Lett.* **80**, 1818 (1998).
- [23] V. A. Kostelecký, *Phys. Rev. D* **64**, 076001 (2001).
- [24] V. A. Kostelecký, *Phys. Rev. D* **61**, 016002 (1999).
- [25] M. Pivk and F. R. Le Diberder, *Nucl. Instrum. Methods Phys. Res., Sect. A* **555**, 356 (2005).
- [26] R. Aaij *et al.* (*LHCb* Collaboration), *Phys. Lett. B* **739**, 218 (2014).
- [27] R. Aaij *et al.* (*LHCb* Collaboration), *Phys. Rev. Lett.* **114**, 041601 (2015).
- [28] J. Scargle, *Astrophys. J.* **263**, 835 (1982).
- [29] J. Horne and S. Baliunas, *Astrophys. J.* **302**, 757 (1986).
- [30] A. Lenz and U. Nierste, *J. High Energy Phys.* **06** (2007) 072.

R. Aaij,³⁹ C. Abellán Beteta,⁴¹ B. Adeva,³⁸ M. Adinolfi,⁴⁷ Z. Ajaltouni,⁵ S. Akar,⁶ J. Albrecht,¹⁰ F. Alessio,³⁹ M. Alexander,⁵² S. Ali,⁴² G. Alkhazov,³¹ P. Alvarez Cartelle,⁵⁴ A. A. Alves Jr,⁵⁸ S. Amato,² S. Amerio,²³ Y. Amhis,⁷ L. An,^{3,40} L. Anderlini,¹⁸ G. Andreassi,⁴⁰ M. Andreotti,^{17,a} J. E. Andrews,⁵⁹ R. B. Appleby,⁵⁵ O. Aquines Gutierrez,¹¹ F. Archilli,³⁹ P. d'Argent,¹² A. Artamonov,³⁶ M. Artuso,⁶⁰ E. Aslanides,⁶ G. Auriemma,^{26,b} M. Baalouch,⁵ S. Bachmann,¹² J. J. Back,⁴⁹ A. Badalov,³⁷ C. Baesso,⁶¹ S. Baker,⁵⁴ W. Baldini,¹⁷ R. J. Barlow,⁵⁵ C. Barschel,³⁹ S. Barsuk,⁷ W. Barter,³⁹ V. Batozskaya,²⁹ V. Battista,⁴⁰ A. Bay,⁴⁰ L. Beaucourt,⁴ J. Beddow,⁵² F. Bedeschi,²⁴ I. Bediaga,¹ L. J. Bel,⁴² V. Bellee,⁴⁰ N. Belloli,^{21,c} I. Belyaev,³² E. Ben-Haim,⁸ G. Bencivenni,¹⁹ S. Benson,³⁹ J. Benton,⁴⁷ A. Berezhnoy,³³ R. Bernet,⁴¹ A. Bertolin,²³ F. Betti,¹⁵ M.-O. Bettler,³⁹ M. van Beuzekom,⁴² S. Bifani,⁴⁶ P. Billoir,⁸ T. Bird,⁵⁵ A. Birnkraut,¹⁰ A. Bizzeti,^{18,d} T. Blake,⁴⁹ F. Blanc,⁴⁰ J. Blouw,¹¹ S. Blusk,⁶⁰ V. Bocci,²⁶ A. Bondar,³⁵ N. Bondar,^{31,39} W. Bonivento,¹⁶ A. Borgheresi,^{21,c} S. Borghi,⁵⁵ M. Borisjak,⁶⁷ M. Borsato,³⁸ M. Boubdir,⁹ T. J. V. Bowcock,⁵³ E. Bowen,⁴¹ C. Bozzi,^{17,39} S. Braun,¹² M. Britsch,¹² T. Britton,⁶⁰ J. Brodzicka,⁵⁵ E. Buchanan,⁴⁷ C. Burr,⁵⁵ A. Bursche,² J. Buytaert,³⁹ S. Cadeddu,¹⁶ R. Calabrese,^{17,a} M. Calvi,^{21,c} M. Calvo Gomez,^{37,e} P. Campana,¹⁹ D. Campora Perez,³⁹ L. Capriotti,⁵⁵ A. Carbone,^{15,f} G. Carboni,^{25,g} R. Cardinale,^{20,h} A. Cardini,¹⁶ P. Carniti,^{21,c} L. Carson,⁵¹ K. Carvalho Akiba,² G. Casse,⁵³ L. Cassina,^{21,c} L. Castillo Garcia,⁴⁰ M. Cattaneo,³⁹ Ch. Cauet,¹⁰ G. Cavallero,²⁰ R. Cenci,^{24,i} M. Charles,⁸ Ph. Charpentier,³⁹ G. Chatzikonstantinidis,⁴⁶ M. Chefdeville,⁴ S. Chen,⁵⁵ S.-F. Cheung,⁵⁶ M. Chrzaszcz,^{41,27} X. Cid Vidal,³⁹ G. Ciezarek,⁴² P. E. L. Clarke,⁵¹ M. Clemencic,³⁹ H. V. Cliff,⁴⁸ J. Closier,³⁹ V. Coco,⁵⁸ J. Cogan,⁶ E. Cogneras,⁵ V. Cogoni,^{16,j} L. Cojocariu,³⁰ G. Collazuol,^{23,k} P. Collins,³⁹ A. Comerma-Montells,¹² A. Contu,³⁹ A. Cook,⁴⁷ M. Coombes,⁴⁷ S. Coquereau,⁸ G. Corti,³⁹ M. Corvo,^{17,a} B. Couturier,³⁹ G. A. Cowan,⁵¹ D. C. Craik,⁵¹ A. Crocombe,⁴⁹ M. Cruz Torres,⁶¹ S. Cunliffe,⁵⁴ R. Currie,⁵⁴ C. D'Ambrosio,³⁹ E. Dall'Occo,⁴² J. Dalseno,⁴⁷ P. N. Y. David,⁴² A. Davis,⁵⁸ O. De Aguiar Francisco,² K. De Bruyn,⁶ S. De Capua,⁵⁵ M. De Cian,¹² J. M. De Miranda,¹ L. De Paula,² P. De Simone,¹⁹ C.-T. Dean,⁵² D. Decamp,⁴ M. Deckenhoff,¹⁰ L. Del Buono,⁸ N. Déléage,⁴ M. Demmer,¹⁰ D. Derkach,⁶⁷ O. Deschamps,⁵ F. Dettori,³⁹ B. Dey,²² A. Di Canto,³⁹ F. Di Ruscio,²⁵ H. Dijkstra,³⁹ F. Dordei,³⁹ M. Dorigo,⁴⁰ A. Dosil Suárez,³⁸ A. Dovbnya,⁴⁴ K. Dreimanis,⁵³ L. Dufour,⁴² G. Dujany,⁵⁵ K. Dungs,³⁹ P. Durante,³⁹ R. Dzhelyadin,³⁶ A. Dziurda,²⁷ A. Dzyuba,³¹ S. Easo,^{50,39} U. Egede,⁵⁴ V. Egorychev,³² S. Eidelman,³⁵ S. Eisenhardt,⁵¹ U. Eitschberger,¹⁰ R. Ekelhof,¹⁰ L. Eklund,⁵² I. El Rifai,⁵ Ch. Elsasser,⁴¹ S. Ely,⁶⁰ S. Esen,¹² H. M. Evans,⁴⁸ T. Evans,⁵⁶ A. Falabella,¹⁵ C. Färber,³⁹

- N. Farley,⁴⁶ S. Farry,⁵³ R. Fay,⁵³ D. Fazzini,^{21,c} D. Ferguson,⁵¹ V. Fernandez Albor,³⁸ F. Ferrari,¹⁵ F. Ferreira Rodrigues,¹ M. Ferro-Luzzi,³⁹ S. Filippov,³⁴ M. Fiore,^{17,a} M. Fiorini,^{17,a} M. Firlej,²⁸ C. Fitzpatrick,⁴⁰ T. Fiutowski,²⁸ F. Fleuret,^{7,l} K. Fohl,³⁹ M. Fontana,¹⁶ F. Fontanelli,^{20,h} D. C. Forshaw,⁶⁰ R. Forty,³⁹ M. Frank,³⁹ C. Frei,³⁹ M. Frosini,¹⁸ J. Fu,²² E. Furfaro,^{25,g} A. Gallas Torreira,³⁸ D. Galli,^{15,f} S. Gallorini,²³ S. Gambetta,⁵¹ M. Gandelman,² P. Gandini,⁵⁶ Y. Gao,³ J. García Pardiñas,³⁸ J. Garra Tico,⁴⁸ L. Garrido,³⁷ P. J. Garsed,⁴⁸ D. Gascon,³⁷ C. Gaspar,³⁹ L. Gavardi,¹⁰ G. Gazzoni,⁵ D. Gerick,¹² E. Gersabeck,¹² M. Gersabeck,⁵⁵ T. Gershon,⁴⁹ Ph. Ghez,⁴ S. Gianì,⁴⁰ V. Gibson,⁴⁸ O. G. Girard,⁴⁰ L. Giubega,³⁰ V. V. Gligorov,³⁹ C. Göbel,⁶¹ D. Golubkov,³² A. Golutvin,^{54,39} A. Gomes,^{1,m} C. Gotti,^{21,c} M. Grabalosa Gándara,⁵ R. Graciani Diaz,³⁷ L. A. Granado Cardoso,³⁹ E. Graugés,³⁷ E. Graverini,⁴¹ G. Graziani,¹⁸ A. Grecu,³⁰ P. Griffith,⁴⁶ L. Grillo,¹² O. Grünberg,⁶⁵ E. Gushchin,³⁴ Yu. Guz,^{36,39} T. Gys,³⁹ T. Hadavizadeh,⁵⁶ C. Hadjivasiliou,⁶⁰ G. Haefeli,⁴⁰ C. Haen,³⁹ S. C. Haines,⁴⁸ S. Hall,⁵⁴ B. Hamilton,⁵⁹ X. Han,¹² S. Hansmann-Menzemer,¹² N. Harnew,⁵⁶ S. T. Harnew,⁴⁷ J. Harrison,⁵⁵ J. He,³⁹ T. Head,⁴⁰ A. Heister,⁹ K. Hennessy,⁵³ P. Henrard,⁵ L. Henry,⁸ J. A. Hernando Morata,³⁸ E. van Herwijnen,³⁹ M. Heß,⁶⁵ A. Hicheur,² D. Hill,⁵⁶ M. Hoballah,⁵ C. Hombach,⁵⁵ L. Hongming,⁴⁰ W. Hulsbergen,⁴² T. Humair,⁵⁴ M. Hushchyn,⁶⁷ N. Hussain,⁵⁶ D. Hutchcroft,⁵³ M. Idzik,²⁸ P. Ilten,⁵⁷ R. Jacobsson,³⁹ A. Jaeger,¹² J. Jalocha,⁵⁶ E. Jans,⁴² A. Jawahery,⁵⁹ M. John,⁵⁶ D. Johnson,³⁹ C. R. Jones,⁴⁸ C. Joram,³⁹ B. Jost,³⁹ N. Jurik,⁶⁰ S. Kandybei,⁴⁴ W. Kanso,⁶ M. Karacson,³⁹ T. M. Karbach,³⁹ S. Karodia,⁵² M. Kecke,¹² M. Kelsey,⁶⁰ I. R. Kenyon,⁴⁶ M. Kenzie,³⁹ T. Ketel,⁴³ E. Khairullin,⁶⁷ B. Khanji,^{21,39,c} C. Khurewathanakul,⁴⁰ T. Kirn,⁹ S. Klaver,⁵⁵ K. Klimaszewski,²⁹ M. Kolpin,¹² I. Komarov,⁴⁰ R. F. Koopman,⁴³ P. Koppenburg,^{42,39} M. Kozeiha,⁵ L. Kravchuk,³⁴ K. Kreplin,¹² M. Kreps,⁴⁹ P. Krokovny,³⁵ F. Kruse,¹⁰ W. Krzemien,²⁹ W. Kucewicz,^{27,n} M. Kucharczyk,²⁷ V. Kudryavtsev,³⁵ A. K. Kuonen,⁴⁰ K. Kurek,²⁹ T. Kvaratskheliya,³² D. Lacarrere,³⁹ G. Lafferty,^{55,39} A. Lai,¹⁶ D. Lambert,⁵¹ G. Lanfranchi,¹⁹ C. Langenbruch,⁴⁹ B. Langhans,³⁹ T. Latham,⁴⁹ C. Lazzeroni,⁴⁶ R. Le Gac,⁶ J. van Leerdam,⁴² J.-P. Lees,⁴ R. Lefèvre,⁵ A. Leflat,^{33,39} J. Lefrançois,⁷ E. Lemos Cid,³⁸ O. Leroy,⁶ T. Lesiak,²⁷ B. Leverington,¹² Y. Li,⁷ T. Likhomanenko,^{67,66} R. Lindner,³⁹ C. Linn,³⁹ F. Lionetto,⁴¹ B. Liu,¹⁶ X. Liu,³ D. Loh,⁴⁹ I. Longstaff,⁵² J. H. Lopes,² D. Lucchesi,^{23,k} M. Lucio Martinez,³⁸ H. Luo,⁵¹ A. Lupato,²³ E. Luppi,^{17,a} O. Lupton,⁵⁶ N. Lusardi,²² A. Lusiani,²⁴ X. Lyu,⁶² F. Machefert,⁷ F. Maciuc,³⁰ O. Maev,³¹ K. Maguire,⁵⁵ S. Malde,⁵⁶ A. Malinin,⁶⁶ G. Manca,⁷ G. Mancinelli,⁶ P. Manning,⁶⁰ A. Mapelli,³⁹ J. Maratas,⁵ J. F. Marchand,⁴ U. Marconi,¹⁵ C. Marin Benito,³⁷ P. Marino,^{24,i} J. Marks,¹² G. Martellotti,²⁶ M. Martin,⁶ M. Martinelli,⁴⁰ D. Martinez Santos,³⁸ F. Martinez Vidal,⁶⁸ D. Martins Tostes,² L. M. Massacrier,⁷ A. Massafferri,¹ R. Matev,³⁹ A. Mathad,⁴⁹ Z. Mathe,³⁹ C. Matteuzzi,²¹ A. Mauri,⁴¹ B. Maurin,⁴⁰ A. Mazurov,⁴⁶ M. McCann,⁵⁴ J. McCarthy,⁴⁶ A. McNab,⁵⁵ R. McNulty,¹³ B. Meadows,⁵⁸ F. Meier,¹⁰ M. Meissner,¹² D. Melnychuk,²⁹ M. Merk,⁴² A. Merli,^{22,o} E. Michielin,²³ D. A. Milanes,⁶⁴ M.-N. Minard,⁴ D. S. Mitzel,¹² J. Molina Rodriguez,⁶¹ I. A. Monroy,⁶⁴ S. Monteil,⁵ M. Morandin,²³ P. Morawski,²⁸ A. Mordà,⁶ M. J. Morello,^{24,i} J. Moron,²⁸ A. B. Morris,⁵¹ R. Mountain,⁶⁰ F. Muheim,⁵¹ D. Müller,⁵⁵ J. Müller,¹⁰ K. Müller,⁴¹ V. Müller,¹⁰ M. Mussini,¹⁵ B. Muster,⁴⁰ P. Naik,⁴⁷ T. Nakada,⁴⁰ R. Nandakumar,⁵⁰ A. Nandi,⁵⁶ I. Nasteva,² M. Needham,⁵¹ N. Neri,²² S. Neubert,¹² N. Neufeld,³⁹ M. Neuner,¹² A. D. Nguyen,⁴⁰ C. Nguyen-Mau,^{40,p} V. Niess,⁵ S. Nieswand,⁹ R. Niet,¹⁰ N. Nikitin,³³ T. Nikodem,¹² A. Novoselov,³⁶ D. P. O'Hanlon,⁴⁹ A. Oblakowska-Mucha,²⁸ V. Obraztsov,³⁶ S. Ogilvy,⁵² O. Okhrimenko,⁴⁵ R. Oldeman,^{16,48,j} C. J. G. Onderwater,⁶⁹ B. Osorio Rodrigues,¹ J. M. Otalora Goicochea,² A. Otto,³⁹ P. Owen,⁵⁴ A. Oyanguren,⁶⁸ A. Palano,^{14,q} F. Palombo,^{22,o} M. Palutan,¹⁹ J. Panman,³⁹ A. Papanestis,⁵⁰ M. Pappagallo,⁵² L. L. Pappalardo,^{17,a} C. Pappenheimer,⁵⁸ W. Parker,⁵⁹ C. Parkes,⁵⁵ G. Passaleva,¹⁸ G. D. Patel,⁵³ M. Patel,⁵⁴ C. Patrignani,^{20,h} A. Pearce,^{55,50} A. Pellegrino,⁴² G. Penso,^{26,r} M. Pepe Altarelli,³⁹ S. Perazzini,^{15,f} P. Perret,⁵ L. Pescatore,⁴⁶ K. Petridis,⁴⁷ A. Petrolini,^{20,h} M. Petruzzo,²² E. Picatoste Olloqui,³⁷ B. Pietrzyk,⁴ M. Pikies,²⁷ D. Pinci,²⁶ A. Pistone,²⁰ A. Piucci,¹² S. Playfer,⁵¹ M. Plo Casasus,³⁸ T. Poikela,³⁹ F. Polci,⁸ A. Poluektov,^{49,35} I. Polyakov,³² E. Polycarpo,² A. Popov,³⁶ D. Popov,^{11,39} B. Popovici,³⁰ C. Potterat,² E. Price,⁴⁷ J. D. Price,⁵³ J. Prisciandaro,³⁸ A. Pritchard,⁵³ C. Prouve,⁴⁷ V. Pugatch,⁴⁵ A. Puig Navarro,⁴⁰ G. Punzi,^{24,s} W. Qian,⁵⁶ R. Quagliani,^{7,47} B. Rachwal,²⁷ J. H. Rademacker,⁴⁷ M. Rama,²⁴ M. Ramos Pernas,³⁸ M. S. Rangel,² I. Raniuk,⁴⁴ G. Raven,⁴³ F. Redi,⁵⁴ S. Reichert,⁵⁵ A. C. dos Reis,¹ V. Renaudin,⁷ S. Ricciardi,⁵⁰ S. Richards,⁴⁷ M. Rihl,³⁹ K. Rinnert,^{53,39} V. Rives Molina,³⁷ P. Robbe,⁷ A. B. Rodrigues,¹ E. Rodriguez Lopez,⁶⁴ P. Rodriguez Perez,⁵⁵ A. Rogozhnikov,⁶⁷ S. Roiser,³⁹ V. Romanovsky,³⁶ A. Romero Vidal,³⁸ J. W. Ronayne,¹³ M. Rotondo,²³ T. Ruf,³⁹ P. Ruiz Valls,⁶⁸ J. J. Saborido Silva,³⁸ N. Sagidova,³¹ B. Saitta,^{16,j} V. Salustino Guimaraes,² C. Sanchez Mayordomo,⁶⁸ B. Sanmartin Sedes,³⁸ R. Santacesaria,²⁶ C. Santamarina Rios,³⁸ M. Santimaria,¹⁹ E. Santovetti,^{25,g} A. Sarti,^{19,r} C. Satriano,^{26,b} A. Satta,²⁵ D. M. Saunders,⁴⁷ D. Savrina,^{32,33} S. Schael,⁹ M. Schiller,³⁹ H. Schindler,³⁹ M. Schlupp,¹⁰ M. Schmelling,¹¹ T. Schmelzer,¹⁰ B. Schmidt,³⁹ O. Schneider,⁴⁰ A. Schopper,³⁹ M. Schubiger,⁴⁰ M.-H. Schune,⁷

R. Schwemmer,³⁹ B. Sciascia,¹⁹ A. Sciubba,^{26,r} A. Semennikov,³² A. Sergi,⁴⁶ N. Serra,⁴¹ J. Serrano,⁶ L. Sestini,²³
 P. Seyfert,²¹ M. Shapkin,³⁶ I. Shapoval,^{17,44,a} Y. Shcheglov,³¹ T. Shears,⁵³ L. Shekhtman,³⁵ V. Shevchenko,⁶⁶ A. Shires,¹⁰
 B. G. Siddi,¹⁷ R. Silva Coutinho,⁴¹ L. Silva de Oliveira,² G. Simi,^{23,s} M. Sirendi,⁴⁸ N. Skidmore,⁴⁷ T. Skwarnicki,⁶⁰
 E. Smith,⁵⁴ I. T. Smith,⁵¹ J. Smith,⁴⁸ M. Smith,⁵⁵ H. Snoek,⁴² M. D. Sokoloff,⁵⁸ F. J. P. Soler,⁵² F. Soomro,⁴⁰ D. Souza,⁴⁷
 B. Souza De Paula,² B. Spaan,¹⁰ P. Spradlin,⁵² S. Sridharan,³⁹ F. Stagni,³⁹ M. Stahl,¹² S. Stahl,³⁹ S. Stefkova,⁵⁴
 O. Steinkamp,⁴¹ O. Stenyakin,³⁶ S. Stevenson,⁵⁶ S. Stoica,³⁰ S. Stone,⁶⁰ B. Storaci,⁴¹ S. Stracka,^{24,i} M. Straticiuc,³⁰
 U. Straumann,⁴¹ L. Sun,⁵⁸ W. Sutcliffe,⁵⁴ K. Swientek,²⁸ S. Swientek,¹⁰ V. Syropoulos,⁴³ M. Szczekowski,²⁹ T. Szumlak,²⁸
 S. T'Jampens,⁴ A. Tayduganov,⁶ T. Tekampe,¹⁰ G. Tellarini,^{17,a} F. Teubert,³⁹ C. Thomas,⁵⁶ E. Thomas,³⁹ J. van Tilburg,⁴²
 V. Tisserand,⁴ M. Tobin,⁴⁰ S. Tolk,⁴³ L. Tomassetti,^{17,a} D. Tonelli,³⁹ S. Topp-Joergensen,⁵⁶ E. Tournefier,⁴ S. Tourneur,⁴⁰
 K. Trabelsi,⁴⁰ M. Traill,⁵² M. T. Tran,⁴⁰ M. Tresch,⁴¹ A. Trisovic,³⁹ A. Tsaregorodtsev,⁶ P. Tsopelas,⁴² N. Tuning,^{42,39}
 A. Ukleja,²⁹ A. Ustyuzhanin,^{67,66} U. Uwer,¹² C. Vacca,^{16,39,j} V. Vagnoni,¹⁵ S. Valat,³⁹ G. Valenti,¹⁵ A. Vallier,⁷
 R. Vazquez Gomez,¹⁹ P. Vazquez Regueiro,³⁸ C. Vázquez Sierra,³⁸ S. Vecchi,¹⁷ M. van Veghel,⁴² J. J. Velthuis,⁴⁷
 M. Veltre,^{18,t} G. Veneziano,⁴⁰ M. Vesterinen,¹² B. Viaud,⁷ D. Vieira,² M. Vieites Diaz,³⁸ X. Vilasis-Cardona,^{37,e} V. Volkov,³³
 A. Vollhardt,⁴¹ D. Voong,⁴⁷ A. Vorobyev,³¹ V. Vorobyev,³⁵ C. Voß,⁶⁵ J. A. de Vries,⁴² R. Waldi,⁶⁵ C. Wallace,⁴⁹ R. Wallace,¹³
 J. Walsh,²⁴ J. Wang,⁶⁰ D. R. Ward,⁴⁸ N. K. Watson,⁴⁶ D. Websdale,⁵⁴ A. Weiden,⁴¹ M. Whitehead,³⁹ J. Wicht,⁴⁹
 G. Wilkinson,^{56,39} M. Wilkinson,⁶⁰ M. Williams,³⁹ M. P. Williams,⁴⁶ M. Williams,⁵⁷ T. Williams,⁴⁶ F. F. Wilson,⁵⁰
 J. Wimberley,⁵⁹ J. Wishahi,¹⁰ W. Wislicki,²⁹ M. Witek,²⁷ G. Wormser,⁷ S. A. Wotton,⁴⁸ K. Wraight,⁵² S. Wright,⁴⁸
 K. Wyllie,³⁹ Y. Xie,⁶³ Z. Xu,⁴⁰ Z. Yang,³ H. Yin,⁶³ J. Yu,⁶³ X. Yuan,³⁵ O. Yushchenko,³⁶ M. Zangoli,¹⁵ M. Zavertyaev,^{11,u}
 L. Zhang,³ Y. Zhang,³ A. Zhelezov,¹² Y. Zheng,⁶² A. Zhokhov,³² L. Zhong,³ V. Zhukov,⁹ and S. Zucchelli¹⁵

(LHCb Collaboration)

¹*Centro Brasileiro de Pesquisas Físicas (CBPF), Rio de Janeiro, Brazil*²*Universidade Federal do Rio de Janeiro (UFRJ), Rio de Janeiro, Brazil*³*Center for High Energy Physics, Tsinghua University, Beijing, China*⁴*LAPP, Université Savoie Mont-Blanc, CNRS/IN2P3, Annecy-Le-Vieux, France*⁵*Clermont Université, Université Blaise Pascal, CNRS/IN2P3, LPC, Clermont-Ferrand, France*⁶*CPPM, Aix-Marseille Université, CNRS/IN2P3, Marseille, France*⁷*LAL, Université Paris-Sud, CNRS/IN2P3, Orsay, France*⁸*LPNHE, Université Pierre et Marie Curie, Université Paris Diderot, CNRS/IN2P3, Paris, France*⁹*I. Physikalisches Institut, RWTH Aachen University, Aachen, Germany*¹⁰*Fakultät Physik, Technische Universität Dortmund, Dortmund, Germany*¹¹*Max-Planck-Institut für Kernphysik (MPIK), Heidelberg, Germany*¹²*Physikalisch-Technische Bundesanstalt (PTB), Braunschweig, Germany*¹³*School of Physics, University College Dublin, Dublin, Ireland*¹⁴*Sezione INFN di Bari, Bari, Italy*¹⁵*Sezione INFN di Bologna, Bologna, Italy*¹⁶*Sezione INFN di Cagliari, Cagliari, Italy*¹⁷*Sezione INFN di Ferrara, Ferrara, Italy*¹⁸*Sezione INFN di Firenze, Firenze, Italy*¹⁹*Laboratori Nazionali dell'INFN di Frascati, Frascati, Italy*²⁰*Sezione INFN di Genova, Genova, Italy*²¹*Sezione INFN di Milano Bicocca, Milano, Italy*²²*Sezione INFN di Milano, Milano, Italy*²³*Sezione INFN di Padova, Padova, Italy*²⁴*Sezione INFN di Pisa, Pisa, Italy*²⁵*Sezione INFN di Roma Tor Vergata, Roma, Italy*²⁶*Sezione INFN di Roma La Sapienza, Roma, Italy*²⁷*Henryk Niewodniczanski Institute of Nuclear Physics Polish Academy of Sciences, Kraków, Poland*²⁸*AGH - University of Science and Technology, Faculty of Physics and Applied Computer Science, Kraków, Poland*²⁹*National Center for Nuclear Research (NCBJ), Warsaw, Poland*³⁰*Horia Hulubei National Institute of Physics and Nuclear Engineering, Bucharest-Magurele, Romania*³¹*Petersburg Nuclear Physics Institute (PNPI), Gatchina, Russia*³²*Institute of Theoretical and Experimental Physics (ITEP), Moscow, Russia*³³*Institute of Nuclear Physics, Moscow State University (SINP MSU), Moscow, Russia*

- ³⁴Institute for Nuclear Research of the Russian Academy of Sciences (INR RAN), Moscow, Russia
³⁵Budker Institute of Nuclear Physics (SB RAS) and Novosibirsk State University, Novosibirsk, Russia
³⁶Institute for High Energy Physics (IHEP), Protvino, Russia
³⁷Universitat de Barcelona, Barcelona, Spain
³⁸Universidad de Santiago de Compostela, Santiago de Compostela, Spain
³⁹European Organization for Nuclear Research (CERN), Geneva, Switzerland
⁴⁰Ecole Polytechnique Fédérale de Lausanne (EPFL), Lausanne, Switzerland
⁴¹Physik-Institut, Universität Zürich, Zürich, Switzerland
⁴²Nikhef National Institute for Subatomic Physics, Amsterdam, The Netherlands
⁴³Nikhef National Institute for Subatomic Physics and VU University Amsterdam, Amsterdam, The Netherlands
⁴⁴NSC Kharkiv Institute of Physics and Technology (NSC KIPT), Kharkiv, Ukraine
⁴⁵Institute for Nuclear Research of the National Academy of Sciences (KINR), Kyiv, Ukraine
⁴⁶University of Birmingham, Birmingham, United Kingdom
⁴⁷H. H. Wills Physics Laboratory, University of Bristol, Bristol, United Kingdom
⁴⁸Cavendish Laboratory, University of Cambridge, Cambridge, United Kingdom
⁴⁹Department of Physics, University of Warwick, Coventry, United Kingdom
⁵⁰STFC Rutherford Appleton Laboratory, Didcot, United Kingdom
⁵¹School of Physics and Astronomy, University of Edinburgh, Edinburgh, United Kingdom
⁵²School of Physics and Astronomy, University of Glasgow, Glasgow, United Kingdom
⁵³Oliver Lodge Laboratory, University of Liverpool, Liverpool, United Kingdom
⁵⁴Imperial College London, London, United Kingdom
⁵⁵School of Physics and Astronomy, University of Manchester, Manchester, United Kingdom
⁵⁶Department of Physics, University of Oxford, Oxford, United Kingdom
⁵⁷Massachusetts Institute of Technology, Cambridge, Massachusetts, United States
⁵⁸University of Cincinnati, Cincinnati, Ohio, United States
⁵⁹University of Maryland, College Park, Maryland, United States
⁶⁰Syracuse University, Syracuse, New York, United States
⁶¹Pontifícia Universidade Católica do Rio de Janeiro (PUC-Rio), Rio de Janeiro, Brazil
(associated with Universidade Federal do Rio de Janeiro (UFRJ), Rio de Janeiro, Brazil)
⁶²University of Chinese Academy of Sciences, Beijing, China
(associated with Center for High Energy Physics, Tsinghua University, Beijing, China)
⁶³Institute of Particle Physics, Central China Normal University, Wuhan, Hubei, China
(associated with Center for High Energy Physics, Tsinghua University, Beijing, China)
⁶⁴Departamento de Física, Universidad Nacional de Colombia, Bogota, Colombia
(associated with LPNHE, Université Pierre et Marie Curie, Université Paris Diderot, CNRS/IN2P3, Paris, France)
⁶⁵Institut für Physik, Universität Rostock, Rostock, Germany (associated with Physikalisches Institut,
Ruprecht-Karls-Universität Heidelberg, Heidelberg, Germany)
⁶⁶National Research Centre Kurchatov Institute, Moscow, Russia
(associated with Institute of Theoretical and Experimental Physics (ITEP), Moscow, Russia)
⁶⁷Yandex School of Data Analysis, Moscow, Russia
(associated with Institute of Theoretical and Experimental Physics (ITEP), Moscow, Russia)
⁶⁸Instituto de Física Corpuscular (IFIC), Universitat de València-CSIC, Valencia, Spain
(associated with Universitat de Barcelona, Barcelona, Spain)
⁶⁹Van Swinderen Institute, University of Groningen, Groningen, The Netherlands
(associated with Nikhef National Institute for Subatomic Physics, Amsterdam, The Netherlands)

^aAlso at Università di Ferrara, Ferrara, Italy.^bAlso at Università della Basilicata, Potenza, Italy.^cAlso at Università di Milano Bicocca, Milano, Italy.^dAlso at Università di Modena e Reggio Emilia, Modena, Italy.^eAlso at LIFAELS, La Salle, Universitat Ramon Llull, Barcelona, Spain.^fAlso at Università di Bologna, Bologna, Italy.^gAlso at Università di Roma Tor Vergata, Roma, Italy.^hAlso at Università di Genova, Genova, Italy.ⁱAlso at Scuola Normale Superiore, Pisa, Italy.^jAlso at Università di Cagliari, Cagliari, Italy.^kAlso at Università di Padova, Padova, Italy.^lAlso at Laboratoire Leprince-Ringuet, Palaiseau, France.^mAlso at Universidade Federal do Triângulo Mineiro (UFTM), Uberaba-MG, Brazil.

ⁿAlso at AGH - University of Science and Technology, Faculty of Computer Science, Electronics and Telecommunications, Kraków, Poland.

^oAlso at Università degli Studi di Milano, Milano, Italy.

^pAlso at Hanoi University of Science, Hanoi, Viet Nam.

^qAlso at Università di Bari, Bari, Italy.

^rAlso at Università di Roma La Sapienza, Roma, Italy.

^sAlso at Università di Pisa, Pisa, Italy.

^tAlso at Università di Urbino, Urbino, Italy.

^uAlso at P. N. Lebedev Physical Institute, Russian Academy of Science (LPI RAS), Moscow, Russia.